Journal of Alloys and Compounds 509 (2011) 2738–2744

Contents lists available at ScienceDirect

Journal of Alloys and Compounds

journal homepage: www.elsevier.com/locate/jallcom

The structural and electric properties of Li- and K-substituted $Bi_{0.5}Na_{0.5}TiO_3$ ferroelectric ceramics

Wenzhong Lu, Ying Wang, Guifen Fan*, Xiaohong Wang, Fei Liang

Department of Electronic Science and Technology, Huazhong University of Science and Technology, 1037 Luoyu Road, Wuhan 430074, PR China

ARTICLE INFO

Article history:
Received 1 June 2010
Received in revised form
27 September 2010
Accepted 10 October 2010
Available online 21 October 2010

PACS:
77.65.Bn
77.84.Dy
77.22.−d

Keywords:
Ceramics
X-ray diffraction
Dielectric response
Diffusion phase transition

ABSTRACT

The structure, dielectric properties and phase transition of lithium and potassium modified $Bi_{0.5}Na_{0.5}TiO_3$ ceramics were investigated widely. The phase transition behavior with respect to changes in composition and temperature was investigated using X-ray diffraction analysis, dielectric and ferroelectric characterizations. The experimental results show that there is a diffusion phase transition in $(Na_{1-x}K_x)_{0.5}Bi_{0.5}TiO_3$ ceramics at T_m and the diffuseness of the phase transition is more obvious for the samples near the morphotropic phase boundary. In $(Na_{1-x}Li_x)_{0.5}Bi_{0.5}TiO_3$ system, due to the space charge polarization induced by ions conductivity, the low frequency permittivity increases so remarkably at high temperature that the peak of maximum permittivity vanishes. The hysteresis loops at different temperatures indicate that there is no existence of anti-ferroelectrics in lithium and potassium modified $Bi_{0.5}Na_{0.5}TiO_3$ ceramics above the depolarization temperature T_d. The depolarization reason is that the tetragonal nonpolar phase occurs and leads to the macro–micro domain transformation at about T_d.

1. Introduction

Lead-based piezoelectric materials based on lead zirconate titanate (PZT) and its multi-component system are widely used for all kinds of piezoelectric devices because of their excellent piezoelectric properties. However, the use of lead-based piezoelectric ceramics has caused serious environmental pollution problems due to the strong toxicity of PbO, which comes from high volatility of PbO during sintering and waste of products containing Pb under ground water. In recent decades, lead-free piezoelectric materials as potential replacement for the widely used lead zirconate titanate have attracted a great deal of research interest.

$Bi_{0.5}Na_{0.5}TiO_3$ (abbreviated as BNT), which is a kind of perovskite-type ferroelectric, has been considered to be a promising candidate for lead-free piezoelectric material owing to its strong ferroelectricity (P_r = 38 μC/cm^2) and high Curie temperature (T_c = 320 °C) [1]. At the same time, BNT has a series of complicated phase transitions [2]. It is a rhombohedral ferroelectric phase at room temperature and can be transformed to a tetragonal paraelectric phase and a cubic paraelectric phase at 320 °C and 520 °C, respectively. The curves of permittivity versus temperature of BNT display a very interesting hump anomaly around 200 °C where the depolarization occurs and the temperature corresponding to dielectric anomaly is defined as T_d. The maximum permittivity occurs at 320 °C which is defined as T_m [3]. From the results of XRD in the literature, there is a rhombohedral–tetragonal existence region for BNT in the range of 200–320 °C and the phase transition is a very slow process [4,5]. For the explanation to the dielectric anomaly of BNT or BNT-based solid solution, some authors suggested that they had undergone a transition from ferroelectric to antiferroelectric phase at the temperature T_d according to the double hysteresis loops [6–8]. However, it has not been confirmed by other experimental measurements that an antiferroelectric phase exists in BNT ceramics at the temperature between T_d and T_m [2].

Recently, most investigations have concentrated on the modifications of BNT in order to improve the piezoelectric properties for piezoelectric and pyroelectric applications [9–11]. According to the matching principle of ions radius, electronegative and electrovalence, some cation dopants have been selected as substitute for A- and B-site of this perovskite material [12–14]. The alkali metal ions of Li^+, Na^+ and K^+ which are in the same group in Periodic Table of Elements have the similar properties. From this point of view, the studies on Li and K substituted BNT solid solution always emphasized on the structure, fabricate method and piezoelectric properties [15–17]. Nevertheless, the physical properties, especially the phase transitions in BNT-based materials play a key

* Corresponding author. Tel.: +86 27 87542594; fax: +86 27 87543134.
E-mail address: hustfgf2009@163.com (G. Fan).

0925-8388/$ – see front matter © 2010 Elsevier B.V. All rights reserved.
doi:10.1016/j.jallcom.2010.10.041

role in deciding the applied condition of high performing materials. Appropriate cation modifications (e.g. Pb^{2+}, alkali-earth Me^{2+}) are likely to influence both the dielectric behavior and the temperature of phase transitions [18,19]. Effects on the dielectric properties and phase transition of Li substituted BNT solid solution have not been reported yet. And the results about the dielectric properties and phase transition of K substituted BNT system have divergence in different reports [20,21]. Hiruma et al. have researched the relationship of the depolarization temperature T_d and the piezoelectric properties in BNT-based ceramics [22–24]. This paper aims at presenting the experimental results and systematic interpretations of the structural, dielectric properties, phase transition and piezoelectric properties of Li and K substituted BNT solid solution.

2. Experimental

The following compositions were prepared in this work:

(a) $Na_{0.5}Bi_{0.5}TiO_3$ or BNT
(b) $(Na_{1-x}Li_x)_{0.5}Bi_{0.5}TiO_3$ or BNLT100x, x = 0–0.2
(c) $(Na_{1-x}K_x)_{0.5}Bi_{0.5}$ TiO_3 or BNKT100x, x = 0–0.26
(d) $(Na_{1-x-y}K_xLi_y)_{0.5}Bi_{0.5}TiO_3$ or BNKLT100x − 100y.

All specimens were prepared with the conventional ceramic fabrication technique. Reagent-grade metal oxides or carbonate powders or oxalate of Bi_2O_3, Na_2CO_3, Li_2CO_3, $(COOK)_2{\cdot}H_2O$, and TiO_2 were used as starting raw materials. All the oxides were mixed by ball milling with zirconia ball and ethanol. Then, the mixtures were calcined at 800–900 °C for 3 h. After calcination, the dried mixtures were added with polyvinyl alcohol as a binder for granulation and pressed to form 15-mm diameter and 1-mm thickness disks. The compacted disks of BNLT system and BNKLT ceramics were sintered at 1040–1120 °C for 2 h in air. The compacted disks of BNKT system were sintered at 1100–1200 °C for 2 h in air. The crystal phase of the sintered ceramics was checked using an X-ray diffractometer (X'pert PRO, Holland).

Silver paste was coated on both sides of the sintered samples and fired at 550 °C in order to form electrodes. The specimens were poled in silicone oil bath with a dc field of 4–5 kV/mm at 60–80 °C for 10 min. The dielectric properties were measured using the Agilent 4294A impedance analyzer at 1 kHz. A standard Sawyer–Tower circuit was used to measure the P–E hysteresis loops at 100 Hz.The temperature was measured by using a system of self-made furnace and temperature recorder with the heating rate of 2 °C/min.

3. Results and discussions

The XRD patterns of the BNKT100x system in the 2θ range of 20–70° are shown in Fig. 1. All the ceramics exhibit a pure perovskite structure and no second phases are detected, which indicates that K^+ has diffused into the BNT lattices. Generally, the symmetry of BNT at room temperature is rhombohedral structure characterized by (0 0 3)/(0 2 1) peaks splitting at around 2θ of 40° and a single peak of (2 0 2) at around 2θ of 46.5°. $Bi_{0.5}K_{0.5}TiO_3$ is perovskite-type structure with tetragonal symmetry at room temperature which is featured with splitting of the (0 0 2)/(2 0 0) peaks at around 2θ of 46.5°. For BNKT100x ceramics, a distinct splitting of the (0 0 3)/(0 2 1) peaks at around 2θ of 40° when $x \leq 0.22$ and a distinct splitting of the (0 0 2)/(2 0 0) peaks at around 2θ of 46.5° when $x \geq 0.16$ can be seen. So, BNKT100x solid solution has rhombohedral–tetragonal morphotropic phase boundary (MPB) in the $Bi_{0.5}K_{0.5}TiO_3$ compositional range of 0.16–22 mol% indicated in Fig. 1. For $x > 0.22$, the BNKT100x system is tetragonal symmetry at room temperature. In addition, the detailed XRD results of BNLT100x ceramics, which have been reported elsewhere by authors [15], indicate that BNLT100x system possesses a pure rhombohedral perovskite structure with the Li amount less than 0.2 but the second phase of $Bi_2Ti_2O_7$ and Li_2O_2 occur at $x > 0.2$. The XRD patterns of the Li and K substituted BNT samples in the 2θ range of 20–70° and 38–50° are shown in Fig. 2. The BNT, BNLT10 and BNKT10 have the same structure with the rhombohedral symmetry. And the BNKT16 and BNKLT16-10 show the coexistence of rhombohedral and tetragonal structure. With further increase of Li content, the BNKLT16-35 shows the cubic structure and accompanies the second phase of $Bi_{1.74}Ti_2O_{6.624}$. In addition, the diffraction peak shifts to higher diffraction angle with lithium substitution. The results indicate that Li substitution decreases the distance of lattice plane of BNT system and reduces anisotropy of the structure symmetry.

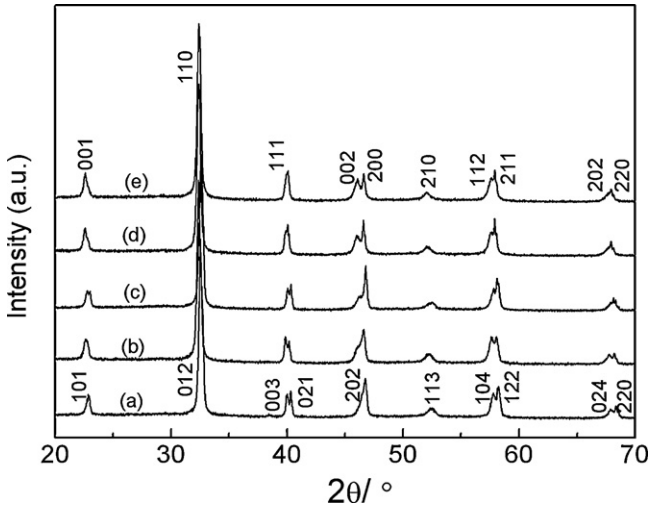

Fig. 1. XRD patterns of the BNKT100x ceramics: (a) x = 0.12; (b) x = 0.16; (c) x = 0.18; (d) x = 0.22; (e) x = 0.26.

Fig. 3 shows the permittivity as a function of temperature and frequency of BNLT100x ceramics. The two dielectric anomalies (maximum permittivity and hump permittivity) are also observed here. As shown in Fig. 3(a)–(c), the dielectric properties of BNLT ceramics at different temperatures and different frequencies are influenced by Li addition remarkably. It is evident that the permittivity exhibits a strongly dependence on the frequency in all measurement temperature range, especially above T_d where the low frequency permittivity increases so rapidly that the peak of maximum permittivity vanishes. With Li content increasing, the phenomenon becomes significant. According to the electrovalence and electronegative matching principle, Li is likely to substitute for Na in the oxygen dodecahedron. The radius of Li ion (0.60 Å), which is so small that it is easy to escape from crystal lattice-site, may become the intersertal ion under thermal excitation. On account of the exponent relation of ionic concentration and temperature, ionic conductivity increases sharply with the increase of temperature. In this way, ionic conductivity has the difference in adjacent Li composition gathering region, which induces the space charge polarization in BNLT ceramics. It is dominative for the space change polarization to contribute to the permittivity at low frequency above T_d. As shown in Fig. 3(d), T_m increases from 315 °C for x = 0 to 445 °C for x = 0.20. T_d is 275 °C for x = 0.06, which is higher than that of pure BNT (205 °C), and then decreases with Li content increasing further and reaches 185 °C for x = 0.20.

Fig. 4 shows the P–E hysteresis loops of BNLT15 ceramics at different temperatures. As the temperature increases, the anisotropy of the structure reduces so that the coercive field E_c and the spontaneous polarization P_s gradually decrease and the reorientation of the domain becomes easy. Therefore, the remanent polarization P_r, which is determined by the P_s and the number of reoriented domain, reaches the maximum value (18 μC/cm^2) at 200 °C, after that the P_r decreases. Above the depolarization temperature T_d (200 °C), the well-hysteresis loop can still be observed. At 230 °C, the circular P–E loop does not have the characteristics of ferroelectric and the BNLT15 ceramic becomes general dielectric. The deformed hysteresis loops are often observed above T_d in BNT-BT solid solution [12]. But in BNLT ceramics, not only the double hysteresis loop but also the "deformed" hysteresis loop is

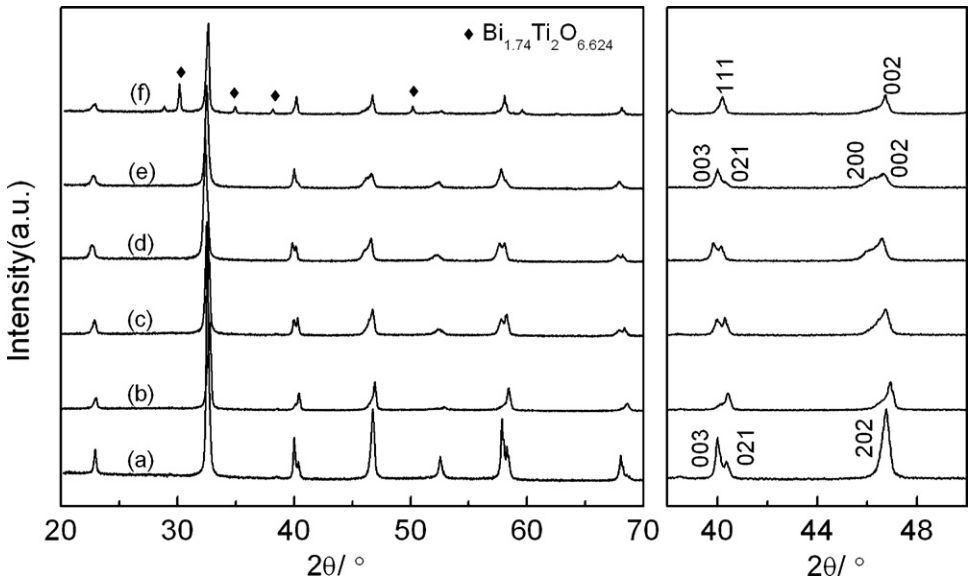

Fig. 2. XRD patterns of Li and K substituted BNT ceramics: (a) BNT, (b) BNLT10, (c) BNKT10, (d) BNKT16, (e) BNKLT16-10, and (f) BNKLT16-35, in the 2θ range of 20–70° and 38–50°.

not observed above T_d. Therefore, the anti-ferroelectric phase in BNLT100x ceramics does not exist above T_d.

Fig. 5 shows the temperature dependence of the permittivity for BNKT100x system at frequencies of 0.1, 1, and 10 kHz on heating. With K content increasing, T_m drops from 315 °C for $x = 0$ to 275 °C for $x = 0.12$ and then rises. T_d decreases from 205 °C for $x = 0$ to 100 °C for $x = 0.26$ (Fig. 5(d)). As shown in Fig. 5(a)–(c), the maximum value of permittivity of BNKT100x ceramics decreases as the measurement frequency increases but the corresponding T_m does not shift towards high temperature. The behavior possesses the characteristics of diffuse phase transition (DPT). At the meantime, the behavior of hump permittivity contains two features in BNKT100x ceramics: (i) a relaxor-like character which means that the permittivity around T_d is dependent on frequency and its temperature of the maximum permittivity shifts upwards with frequency increasing, (ii) spontaneous relaxor-to-ferroelectric-phase transition, which presents the transition of frequency dependence to frequency independence of permittivity in ε (T) curves, occurs in the BNKT100x ($0 < x < 0.22$) ceramics with rhombohedral or rhombohedral–tetragonal symmetry at room temperature

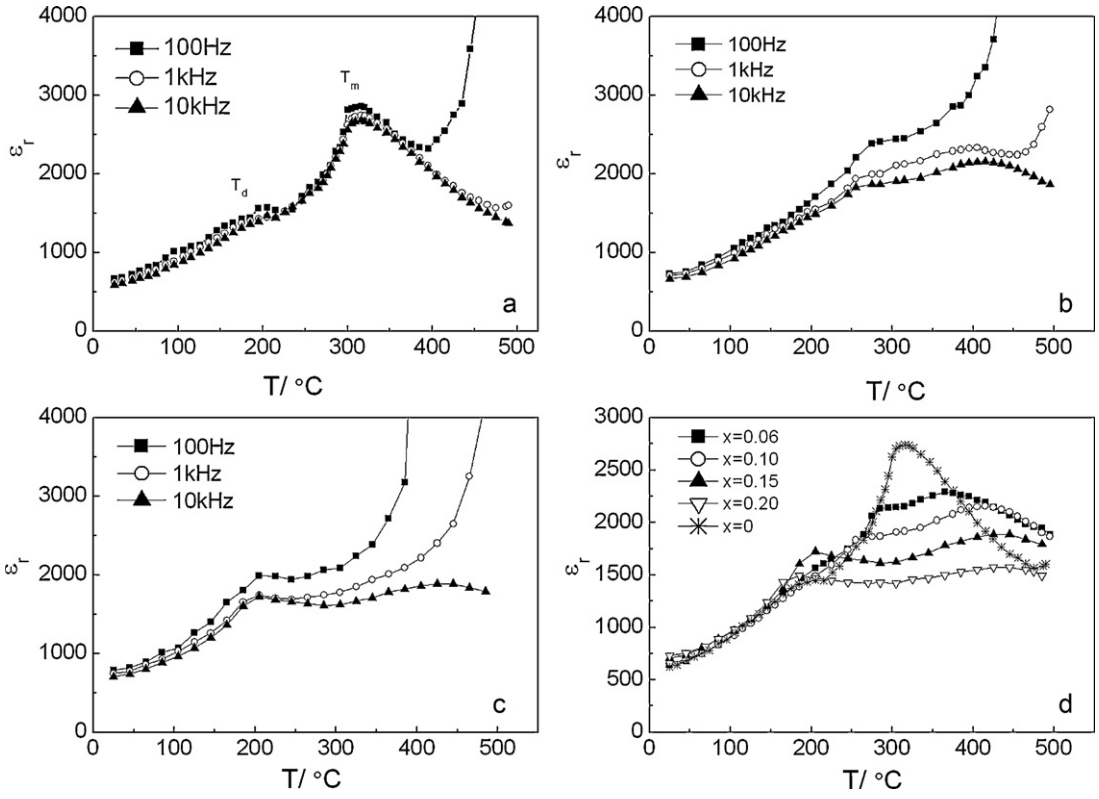

Fig. 3. Temperature dependences of dielectric constant for the unpoled BNLT100x ceramics: (a) $x = 0$, (b) $x = 0.1$, (c) $x = 0.15$, and (d) $x = 0$–0.2, at 10 kHz.

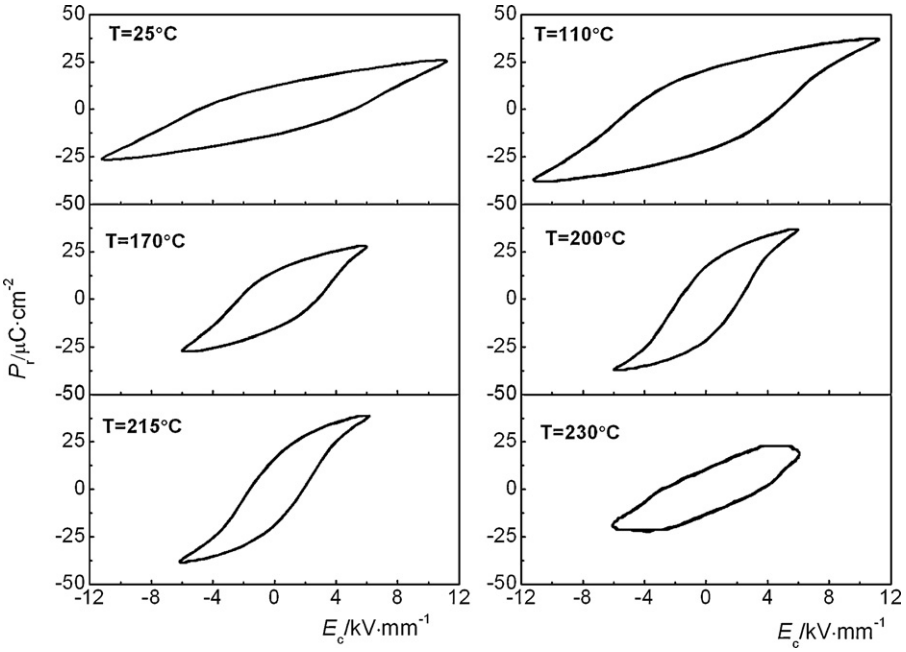

Fig. 4. *P–E* hysteresis loops of BNLT15 ceramics at different temperatures.

(see Fig. 5(a) and (b)). Spontaneous relaxor-to-ferroelectric-phase transition is corresponding with the micro-to-macro-domain transition in Pb-based relaxor ferroelectric [25,26]. The behavior is also observed in BNT-BT system or $Pb(Ni_{1/3}Nb_{1/3})O_3$–$PbTiO_3$–$PbZrO_3$ system with rhombohedral structure [27,28]. Therefore, spontaneous relaxor-to-ferroelectric-phase transition in BNT-based ceramics is correlated with the structure of sample at room temperature. As the literatures have reported, the BNT-based samples with rhombohedral symmetry at room temperature will generate rhombohedral–tetragonal transition around T_d [2]. The internal stress brought by the rhombohedral–tetragonal transition is the driving force of the micro-to-macro-domain transition, which is the cause of spontaneous relaxor-to-ferroelectric-phase transition.

A modified Curie–Weiss law has been proposed to describe the diffuseness of a phase transition at T_m [13]:

$$\frac{1}{\varepsilon} - \frac{1}{\varepsilon_m} = \frac{(T - T_m)^\gamma}{C} \quad (1)$$

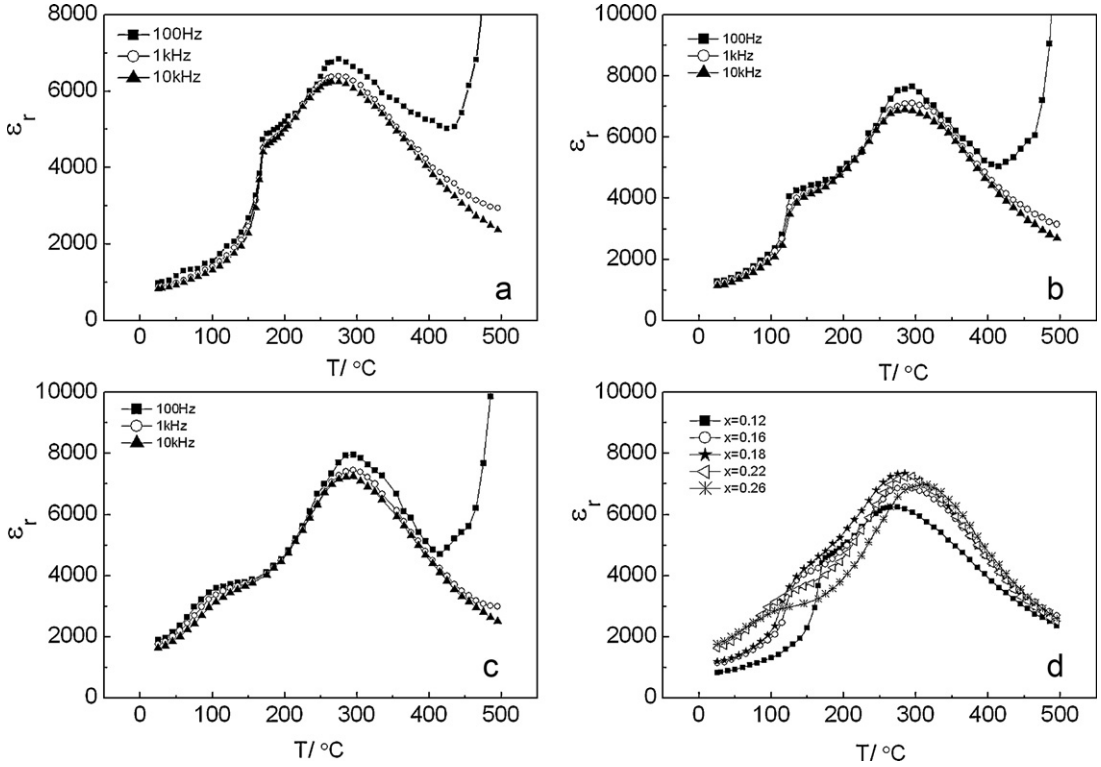

Fig. 5. The temperature dependence of the permittivity for BNK100*x* system: (a) *x* = 0.12, (b) *x* = 0.16, (c) *x* = 0.22, and (d) *x* = 0–0.3, at 10 kHz.

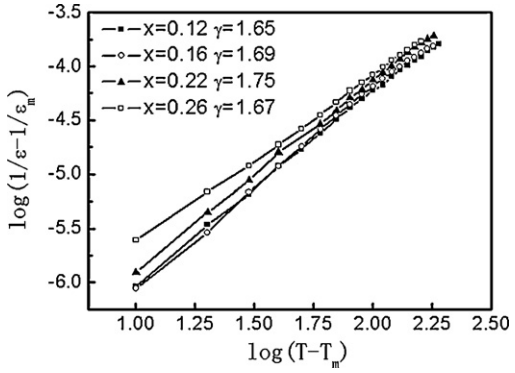

Fig. 6. The plots of $\log(1/\varepsilon - 1/\varepsilon_m)$ as a function of $\log(T - T_m)$ for the BNKT100x ceramics.

where γ is constants for diffusion factor and C means Curie–Weiss constant, respectively. In general, the diffusion factor of γ is between 1 and 2, representing the normal ferroelectric phase transition and completed diffusion phase transition [14]. In the case of $\gamma = 1$, a normal Curie–Weiss law is obtained. The diffusion factor can be employed to describe the diffusion phase transition. The plots of $\log(1/\varepsilon - 1/\varepsilon_m)$ as a function of $\log(T - T_m)$ for the BNKT100x ceramics are shown in Fig. 6. The diffusion factor increases from 1.65 for $x = 0.10$ to the maximum value of 1.75 for $x = 0.22$ and then decreases to 1.67 for $x = 0.26$. The results show that the diffuseness of the phase transition is high for the samples near the MPB in BNKT100x system.

Fig. 7 shows the P–E hysteresis loops of BNKT12 and BNKT26 ceramics at different temperatures. For BNKT12 ceramic, the well-hysteresis loop can be observed when $T \leq 200\,^{\circ}C$. Above 220 °C, the deformed P–E loops which can also be called a "waist" hysteresis loop appear. But for BNKT26 ceramics, the deformed P–E loop does not appear in the range of the measurement temperature. It can be confirmed that there is no anti-ferroelectric phase in BNKT26 ceramics at temperature between T_d and T_m where the rhombohedral and tetragonal coexist. What leads to the deformation of P–E loop for BNKT12 ceramics on heating? According to the result of dielectric properties in BNKT12 ceramic, the T_d is 175 °C. However, the BNKT12 still presents the normal P–E loop at 200 °C and the deformed P–E loop appears at 220 °C. This result does not support the view that the rhombohedral structure in BNT above T_d is an anti-ferroelectric [6].

At room temperature, BNKT12 ceramic is rhombohedral symmetry and BNKT26 ceramics is tetragonal symmetry. So the deformation of P–E loop for BNKT12 ceramics is related to the rhombohedral–tetragonal structure transition on heating. The dielectric anomaly in BNKT12 ceramic near T_d possesses the characteristics of relaxor ferroelectric which is explained by the macro–micro domains switching in Pb-based perovskite structure. The macro–micro domains switching [29,30], which makes the domain size small and the domain wall increasing, leads to changes in electric properties, e.g. the dispersion of permittivity, the permittivity dependence on frequency and depolarization. Furthermore, the strong electric field may transform the micro-domain to macro-domain. The macro–micro domains switching in BNKT ceramics is concerned with the structural phase transition from rhombohedral polar phase to tetragonal nonpolar phase. The change of the hysteresis loop shape of BNKT ceramics at different temperatures is very similar to that of the typical relaxor ferroelectrics such as $Pb(Sc_{0.5}Ta_{0.5})O_3$ [31] and $Pb(Sc_{0.5}Nb_{0.5})O_3$ [32]. The deformed P–E loops are explained by the common effect of the interaction of rhombohedral polar and tetragonal nonpolar phase, which coexist and have the average free energy close to each other and transform each other, and the electric field.

BNKT26 ceramics is a tetragonal ferroelectric while the dielectric anomaly at 100 °C illustrates the existence of rhombohedral phase at room temperature. The rhombohedral phase is so small that the XRD cannot be detected. On heating, the little rhombohedral ferroelectric phase can be transformed to the tetragonal

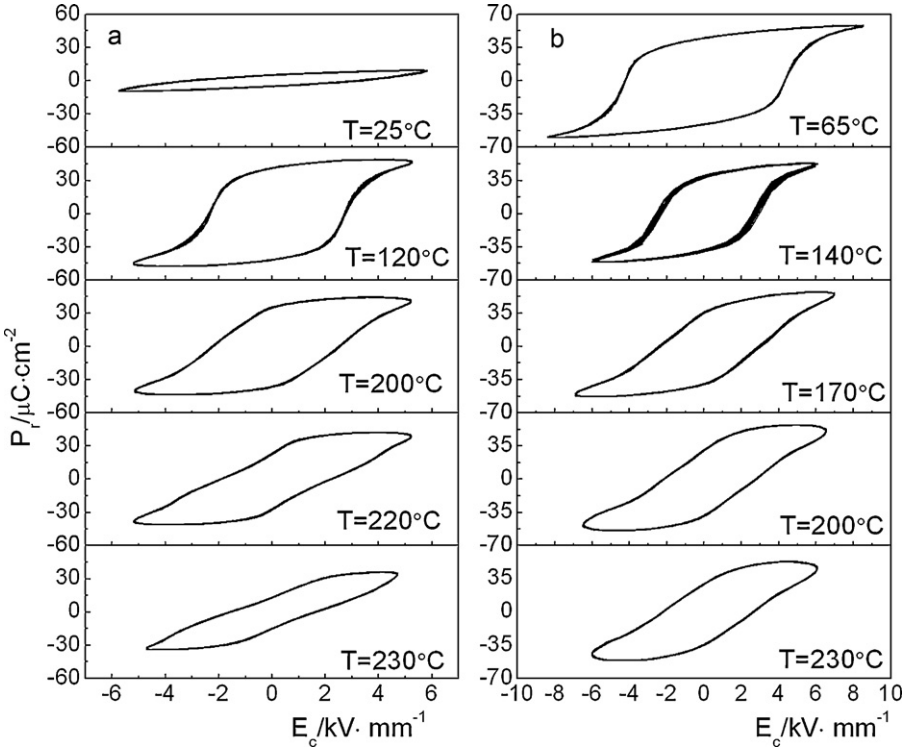

Fig. 7. P–E hysteresis loops of BNKT100x ceramics at different temperatures: (a) BNKT12; (b) BNKT26.

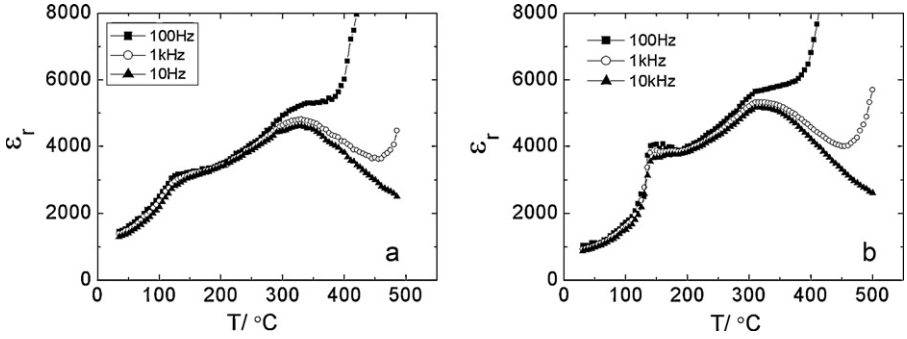

Fig. 8. Temperature and frequency dependences of dielectric constant for BNKLT16-10 ceramics: (a) unpoled; (b) poled.

phase. The force of the rhombohedral–tetragonal phase transition is so small that it cannot make the macro-domain to switch to micro-domain. Therefore, the deformed *P–E* loop cannot be caused at high electric field. As mentioned before, BNLT100*x* ceramics are rhombohedral symmetry at room temperature. But above T_d, the deformed *P–E* loop does not appear. This mainly results from the spontaneous polarization P_s decreasing and the coupling of oxygen octahedral reducing with lower Li replacement. When the tetragonal non-polar phase increases at the high temperature, the strong electric field is not sufficient to make polar micro-region switch into a macro-domain. So the deform loop cannot be observed. In short, the deformed hysteresis loop in BNT-based ceramics when heating is related to the rhombohedral polar phase to tetragonal nonpolar phase transition.

Fig. 8 shows the temperature and frequency dependences of permittivity for poled or unpoled BNKLT16-10 ceramics. As shown in Fig. 8(a) for unpoled BNKLT16-10 ceramics, the permittivity feature of BNKLT ceramics is intervenient between BNKT and BNLT ceramics. The behavior of hump permittivity presents the relaxor-like character. After polarization, the behavior of hump permittivity exhibits relaxor-to-ferroelectric-phase transition character (Fig. 8(b)). The poled field does not change the value of T_m and makes T_d increase from 125 °C to 145 °C. The poled field is the driving force of the micro-to-macro-domain transition and strengthens the domain stability and improves the macro-to-micro-domain transition temperature. At the same time, the permittivity for poled sample is larger than that of unpoled sample at the temperature between T_d and T_m. The enlargement of domain under the high electric field is contributed to the permittivity in this temperature range. Thereby, these results once again evidence the existence of the macro-to-micro-domain transition at T_d which is the cause of the depolarization.

Fig. 9 shows the temperature dependences of permittivity for Li and K substituted BNT ceramics at frequency of 10 kHz on heating. The permittivity of K doped BNT ceramics is larger than that of BNT in the range of measurement temperature, especially the maximum permittivity. However, the permittivity of Li doped BNT ceramics is similar to pure BNT under T_d but is less than that of BNT above T_d. For ferroelectrics, the spontaneous polarization in domain is the main contribution to the permittivity. The radius of

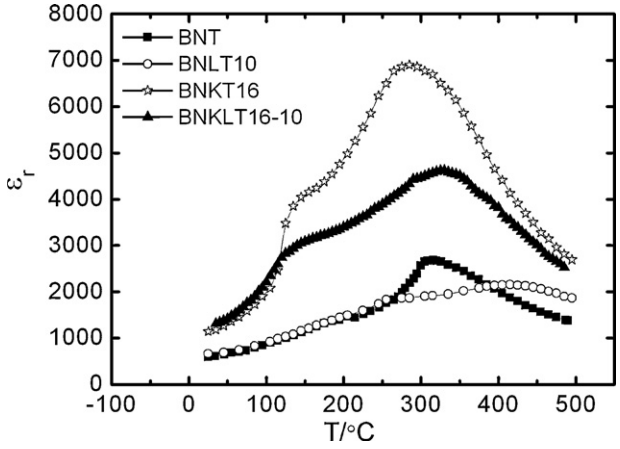

Fig. 9. Temperature dependences of permittivity for Li and K substituted BNT ceramics at frequency of 10 kHz on heating.

K^+ (1.33 Å) is larger than that of Na^+ (1.02 Å). According to XRD data mentioned above, K^+ substituted for Na^+ and occupied the oxygen dodecahedron coordinated site will make the crystal cell enlarged and enhances the coupling of TiO_6 octahedron and makes the spontaneous polarization increase. In addition, the ionic displacement polarization is also beneficial to the permittivity, which is in the ascendant in non-ferroelectric phase. On the contrary, the spontaneous polarization in domain and the ionic displacement polarization in Li doped BNT ceramics are both lower than those of pure BNT.

The dielectric and piezoelectric properties of the typical compositions of Li and K substituted BNT ceramics at room temperature are shown as Table 1. Li and/or K replacement for Na in BNT are beneficial to improve the dielectric and piezoelectric properties, especially for the compositions near the MPB. For BNTKLT16-10, the piezoelectric constant d_{33} and electromechanical coupling coefficient k_p are 160 pC/N and 0.35, respectively, which have a greater improvement compared with the pure BNT ceramics. K substitution for Na in BNT makes the T_d decrease but Li substitution makes the T_m increase in the measurement composition range.

Table 1
Room-temperature dielectric and piezoelectric properties of BNT-based ceramics.

Compositions	BNT	BNLT10	BNKT10	BNKT16	BNKLT16-10
Piezoelectric constant d_{33} (pC/N)	78	95	105	138	160
Electromechanical coupling coefficient (k_p)	0.16	0.18	0.25	0.30	035
Dielectric permittivity ε_r at 25 °C, 1 kHz	420	480	521	1020	1080
Dielectric loss tan δ at 25 °C, 1 kHz	0.03	0.036	0.023	0.029	0.038
Depolarization temperature, T_d (°C)	205	245	175	135	125
Curie temperature, T_m (°C)	315	365	285	295	335

4. Conclusion

The phase transition behavior with respect to changes in composition and temperature was investigated using X-ray diffraction analysis, dielectric and ferroelectric characterizations. The results of XRD show that all patterns of BNKT100x ceramics (x = 0–0.26) exhibit a single perovskite phase. In $\varepsilon(T)$ curves, K lowers the phase transition temperature and makes the maximum permittivity increase. K-substituted BNT presents the character of the diffuse phase transition at T_m and the spontaneous relaxor-to-ferroelectric-phase transition around T_d. On the contrary, Li increases the phase transition temperature and makes the maximum permittivity decrease. Due to the space charge polarization induced by ions conductivity, the low frequency permittivity increases so remarkably at high temperature that the peak of maximum permittivity vanishes. The hysteresis loops at different temperatures indicate that there is no existence of antiferroelectrics in lithium and potassium modified $Bi_{0.5}Na_{0.5}TiO_3$ ceramics above the depolarization temperature T_d. The permittivity feature of BNKLT ceramics is intervenient between BNKT and BNLT ceramics.

Acknowledgements

This work was supported by the Analytical and Testing Centre of HuaZhong University of Science and Technology, by the program for New Century Excellent Talent in University (NCET-07-0329) and Natural Science Foundation of Hubei Province (2008CDB283).

References

[1] G.A. Smolenskii, V.A. Isupov, A.I. Agranovskaya, N.N. Krainik, Sov. Phys. Solid State 2 (1961) 2651.
[2] J. Suchanicz, Ferroelectrics 209 (1998) 561.
[3] S. Senda, J.P. Mercurio, J. Eur. Ceram. Soc. 21 (2001) 1333.
[4] J. Suchanicz, Ferroelectrics 190 (1997) 77.
[5] J. Suchanicz, Ferroelectrics 200 (1997) 319.
[6] V.A. Isupov, I.P. Pronin, et al., Ferroelectrics Lett. 2 (1984) 205.
[7] X.X. Wang, H.L.W. Chan, C.L. Choy, Appl. Phys. A 80 (2005) 333.
[8] H. Nagata, T. Takenaka, J. Eur. Ceram. Soc. 21 (2001) 1299.
[9] M. Chen, Q. Xu, H.K. Bok, et al., J. Eur. Ceram. Soc. 28 (2008) 843.
[10] H. Ishii, H. Nagata, T. Takenaka, Jpn. J. Appl. Phys. 40 (2001) 5560.
[11] Y.M. Li, W. Wen, J. Zhou, Q. Xu, Mater. Sci. Eng. 112 (2004) 5.
[12] D.M. Lin, K.W. Kwok, H.W.L. Chan, J. Phys. D: Appl. Phys. 40 (2007) 5344.
[13] H.Y. Tian, D.Y. Wang, D.M. Lin, J.T. Zeng, et al., Solid State Commun. 142 (2007) 10.
[14] K.K. Lily, K. Prasad, R.N.P. Choudhary, J Alloys Compd 453 (1–2) (2008) 325.
[15] W.Z. Lu, G.F. Fan, X.H. Wang, F. Liang, Jpn. J. Appl. Phys. 450 (11) (2006) 8763.
[16] A. Sasaki, T. Chiba, Y. Mamaiya, Jpn. J. Appl. Phys. 38 (1999) 5564.
[17] F. Gao, C.S. Zhang, X.C. Liu, L.H. Cheng, et al., J. Eur. Ceram. Soc. 27 (2007) 3453.
[18] S. Kuharuangrong, Ceram. Int. 33 (2007) 1403.
[19] J.R. Gomah-Pettry, S. Senda, P. Marchet, J.P. Mercurio, J. Eur. Ceram. Soc. 24 (2004) 1165.
[20] S.C. Zhao, G.D. Li, A.L. Ding, T.B. Wang, J. Phys. D: Appl. Phys. 39 (2006) 2277.
[21] Z.P. Yang, B. Liu, L.L. Wei, Y.T. Hou, Mater. Res. Bull. 43 (2008) 81.
[22] Y. Hiruma, K. Yoshii, H. Nagata, T. Takenaka, J. Appl. Phys. 103 (2008) 084121.
[23] Y. Hiruma, H. Nagata, T. Takenaka, J. Appl. Phys. 104 (2008) 124106.
[24] Y. Hiruma, H. Nagata, T. Takenaka, Ceram. Int. 35 (1) (2009) 117–120.
[25] X.H. Dai, A. Digiiovanni, D. Viehland, J. Appl. Phys. 74 (5) (1993) 3399.
[26] F. Chu, N. Setter, A.V. Tagantsev, J. Appl. Phys. 74 (8) (1993) 5129.
[27] T. Oh, M.-H. Kim, Mater. Sci. Eng. B 132 (2006) 239.
[28] M.S. Yoon, H.M. Jang, J. Appl. Phys. 77 (8) (1995) 3991.
[29] X. Yao, Z.L. Chen, L.E. Cross, J. Appl. Phys. 54 (6) (1983) 3399.
[30] B.J. Chu, D.R. Chen, G.R. Li, Q.R. Yin, J. Eur. Ceram. Soc. 22 (2002) 2115.
[31] F. Chu, N. Setter, J. Appl. Phys. 74 (8) (1993) 5129.
[32] F. Chu, I.M. Reaney, N. Setter, J. Appl. Phys. 77 (4) (1995) 1671.